

“All-Three-in-One”: A New Bismuth–Tellurium–Borate Bi_3TeBO_9 Exhibiting Strong Second Harmonic Generation Response

Mingjun Xia,[†] Xingxing Jiang,[†] Zheshuai Lin,^{*,†,‡} and Rukang Li^{†,‡}

[†]Beijing Center for Crystal Research and Development, Key Laboratory of Functional Crystals and Laser Technology, Technical Institute of Physics and Chemistry, Chinese Academy of Sciences, Beijing 100190, China

[‡]University of Chinese Academy of Sciences, Beijing 100049, China

S Supporting Information

ABSTRACT: A new nonlinear optical (NLO) material, Bi_3TeBO_9 (BTBO), is successfully grown from high temperature solution method. BTBO crystallizes in a polar space group of $P6_3$ with a framework structure composed of $[\text{Bi}_3\text{O}_9]$ blocks, with TeO_6 and BO_3 interconnection. It is interesting that in the BTBO structure three types of NLO-active units, including stereochemically active lone pair cations (Bi^{3+} cations), second-order Jahn–Teller distorted octahedra (TeO_6 octahedra) and π -orbital planar groups (BO_3 groups), simultaneously exist. The additive contribution from these three types of groups results in an extremely large second harmonic generation (SHG) response in BTBO (about 20 times that of KDP), exhibiting the largest SHG effect among the known borate NLO materials. The enhancement of the nonlinear optical property is elucidated by the first-principles analysis.

Lasers with different wavelengths are widely employed in various fields of optoelectronics, such as remote communication, laser medicine, micromanufacturing, and semiconductor photolithograph.^{1,2} Harmonic generation by utilizing the nonlinear optical (NLO) crystals is the most effective technique to tune the frequency of a laser which usually operates with a definite wavelength.³ During the past decades, some commercial NLO crystals have been developed in the spectral ranges from infrared (IR), visible, ultraviolet (UV) to deep UV region, e.g., AgGaX_2 ($X = \text{S}, \text{Se}$),^{4,5} ZnGeP_2 ,⁶ KH_2PO_4 (KDP),⁷ KTiOPO_4 ,⁸ $\beta\text{-BaB}_2\text{O}_4$ (BBO),⁹ LiB_3O_5 (LBO),¹⁰ $\text{CsLiB}_6\text{O}_{10}$ (CLBO),¹¹ $\text{KBe}_2\text{BO}_3\text{F}_2$ (KBBF),¹² etc. It is well-known that the second harmonic generation (SHG) effect is one of the key parameters to characterize the performance of a NLO material because it determines the conversion efficiency of the fundamental laser. So, the exploration for the NLO crystals with large SHG response has been a long-term task, but remains challenging.

A prerequisite for a NLO crystal is that it must possess a noncentrosymmetric (NCS) structure. Traditionally, various strategies were adopted for designing and exploring new NCS materials with large NLO response. A successful design idea is to introduce one or combination of the NLO-active units, including second-order Jahn–Teller (SOJT) distorted MO_6 octahedra ($M = \text{Ti}^{4+}, \text{Nb}^{5+}, \text{Ta}^{5+}, \text{Mo}^{6+}, \text{W}^{6+}, \text{Te}^{6+}$, etc.), stereochemically active lone pair (SCALP) cations ($\text{Pb}^{2+}, \text{Bi}^{3+}$,

$\text{Te}^{4+}, \text{I}^{5+}$, etc.), or π -orbital anionic groups ($\text{BO}_3, \text{B}_3\text{O}_6, \text{NO}_3, \text{CO}_3$, etc.)^{13–15} into the crystal structure. To date, quite a few NCS materials containing one or two NLO-active units with large SHG responses have been reported, e.g., $\text{RbNb}(\text{BO}_3)_2$,¹⁶ Dugganite-type $\text{Pb}_3\text{M}_3\text{NX}_2\text{O}_{14}$ ($M = \text{Mg}, \text{Zn}, \text{N} = \text{Te}, \text{W}$, and $X = \text{P}, \text{V}$),¹⁷ BaTeM_2O_9 ($M = \text{Mo}, \text{W}$),¹⁸ $\text{Li}_2\text{Ti}(\text{IO}_3)_6$,¹⁹ $\text{BaNbO}(\text{IO}_3)_5$,²⁰ APbCO_3F ($A = \text{Rb}, \text{Cs}$).²¹ We speculated that a NLO material may exhibit even stronger SHG response if all of the above three types of NLO active units coexist in one structure. Guided by this idea, we successfully discovered a new NLO crystal Bi_3TeBO_9 (BTBO) with the three types of NLO-active units presented in a structure, thus exhibiting the SHG intensity of 20 times that of KDP, which presents the largest SHG coefficient among the borates NLO materials. In this communication, we report the synthesis, crystal structure, electronic structure, and optical properties of BTBO by combination of experiments and first-principles calculations.

The polycrystalline powder of BTBO was prepared from the stoichiometric mixture of Bi_2O_3 , TeO_2 , and H_3BO_3 by high temperature solid state reaction technique. The mixture was ground thoroughly and preheated at 500 °C for 12 h to decompose water, and finally calcined at 700 °C for 24 h with several intermediate grindings. The phase purities were checked by powder X-ray diffraction (PXRD) refinement (Figure 1). BTBO crystals were successfully grown by high temperature solution method using $\text{TeO}_2\text{-B}_2\text{O}_3$ flux. The mixture with polycrystalline BTBO (90.94 g, 0.1 mol), TeO_2 (7.98g, 0.05

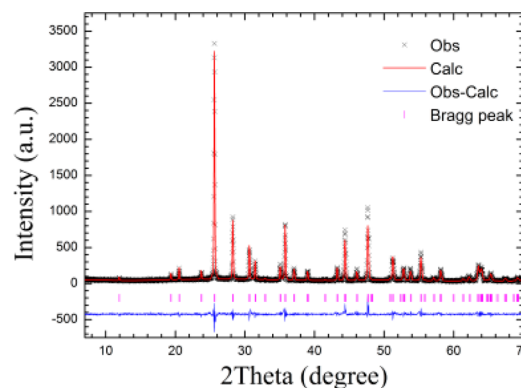


Figure 1. Rietveld refinement plot of the PXRD data for BTBO.

Received: August 23, 2016

Published: October 14, 2016

mol), and H_3BO_3 (6.18g, 0.1 mol) (at a molar ratio of $\text{BTBO}:\text{TeO}_2:\text{B}_2\text{O}_3 = 2:1:1$) was thoroughly ground and placed into a $\Phi 40 \times 40$ cm Pt crucible. The crucible was heated to 800°C in a temperature-programmable electric resistive furnace and held for 24 h to melt completely. The temperature was then decreased to 600°C at a cooling rate of 5°C h^{-1} before the furnace was switched off. Some small crystals of BTBO were obtained by washing away the matrix with hot water.

Single crystal X-ray diffraction revealed that BTBO crystallizes in a polar hexagonal space group of $P6_3$ (No. 173) with the unit cell parameters of $a = 8.7510(12) \text{ \AA}$, $c = 5.8981(12) \text{ \AA}$, and $Z = 2$ (Tables S1–3). As shown in Figure 2,

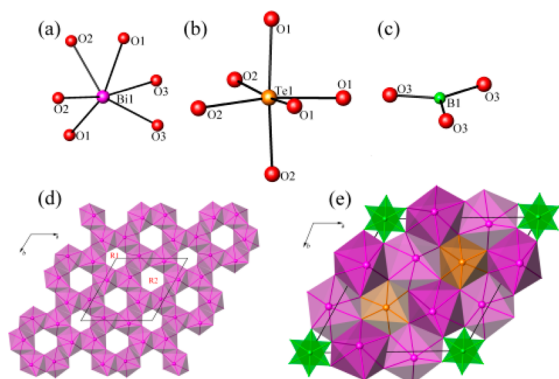


Figure 2. Crystal structure of BTBO: (a) BiO_6 octahedron; (b) distorted TeO_6 octahedron; (c) planar BO_3 group; (d) $[\text{Bi}_6\text{O}_{18}]$ block with two type of cavities; (e) three-dimensional framework.

BTBO features a complicated three-dimensional framework composed of the distorted BiO_6 and TeO_6 octahedra and planar BO_3 groups through corner or edge-sharing interconnection. In the distorted BiO_6 octahedra, Bi^{3+} cations are coordinated by six O atoms with three shorter Bi–O bond lengths of $2.214(7)$ – $2.267(7) \text{ \AA}$ and three longer Bi–O bond distances of $2.505(7)$ – $2.514(7) \text{ \AA}$, presenting the stereochemically active lone pair electrons of Bi^{3+} nearly along the c -axis, as also confirmed by the bond valence sums (BVS) value of 2.96 on Bi ions. Six BiO_6 octahedra are further linked via corner-sharing to form $[\text{Bi}_6\text{O}_{18}]$ blocks that build two types of cavities of R1 and R2 running along the c -axis. Te^{6+} cations are also bonded to six O atoms with two groups with three equal distances of $1.921(7) \text{ \AA}$ and $1.924(7) \text{ \AA}$, but the TeO_6 polyhedra are just slightly deformed from the regular octahedral shape, which are very different with the BiO_6 octahedra. In the TeO_6 octahedra, the Te^{6+} cations are displaced along the 3-fold axis, and thus resulting in a SOJT distortion. The TeO_6 octahedra are filled in the R2 cavities with the connection of O1 and O2 atoms, resulting in the BVS value of 5.91 on Te ions, in accordance with the reported values.¹⁷ B atoms are surrounded by three O3 atoms to form the planar BO_3 groups with a uniform B–O bond length of $1.378(6) \text{ \AA}$. The BO_3 groups with π -orbitals connect the $[\text{Bi}_6\text{O}_{18}]$ blocks via the O3 atoms and accommodate into the R1 tunnels. The IR spectroscopy on BTBO revealed that the peaks located at 1250 cm^{-1} and around 500 – 700 cm^{-1} are ascribed to asymmetric stretching and bending vibrations of the BO_3 group, respectively²² (Figure S1).

Differential scanning calorimetry (DSC) measurement exhibits two endothermic peaks around 828 and 879°C in

the heating curve and one sharp exothermic peak around 793°C in cooling curve, revealing that BTBO melts incongruently (Figure S2). PXRD patterns on the residues indicate that BTBO decomposes to Bi_2TeO_5 after melting, further confirming that BTBO undergoes incongruent melting (Figure S3).

The NLO response in BTBO was measured by the Kurtz–Perry method,²³ which reveals that BTBO is phase-matchable at 1064 nm (Figure 3 and Figure S4). The SHG intensity of

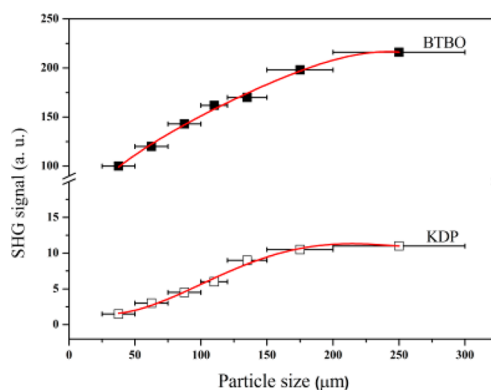


Figure 3. Phase-matching curve for BTBO (KDP samples as reference). The red solid curves are drawn to guide the eyes, not fits to the data.

BTBO is about 20 times that of KDP, presenting the largest SHG effect among the borate NLO crystals (see Table S4). The first-principles calculations based on the density functional theory (DFT)²⁴ show that the independent SHG coefficients in BTBO are $d_{15} = 0.81 \text{ pm/V}$ and $d_{33} = 5.10 \text{ pm/V}$, and the powder SHG effect is $\sim 13 \times$ KDP, in good agreement with the experimental result.

To understand the origin of the large SHG response of BTBO, we performed the structure–property relationship analysis based on the first-principles calculations. The optical property is mainly related to the electron transition near the forbidden band edge.²⁵ The electron structure of BTBO (Figures S5 and S6 and Discussion S1) shows that the orbitals of all the constitute element occupied both the top of valence bands and bottom of conduction bands, indicating that the large SHG response arise from the coexistence of the three types of NLO-active units. To further evaluate quantitatively the contribution of the three types of NLO-active groups to whole SHG coefficients, the real-space atom-cutting analysis²⁶ was adopted (Table 1). It is clearly shown that all the three groups have considerable SHG effect and their additive contribution results in the very large SHG effect in BTBO. Moreover, the contribution of SHG responses from TeO_6 and BiO_6 tetrahedra is much larger than that of BO_3 triangles. Combined with the fact that the number ratio among BiO_6 ,

Table 1. First-Principles Anisotropic SHG Coefficients (pm/V) and the Contribution of the Constituent NLO Active Units Calculated by the Real-Space Atom-Cutting Method

	all	BiO_6	TeO_6	BO_3
d_{33}	5.10	4.68	2.17	0.98
d_{33}/group		1.56	2.17	0.98
d_{15}	0.81	0.51	0.50	0.15
d_{15}/group		0.17	0.50	0.15

TeO₆, and BO₃ groups in BTBO is 3:1:1, one may easily obtain that the large SHG response of BTBO mainly originates from the high number proportion of TeO₆ and BiO₆ with large NLO susceptibility. This conclusion can be also intuitively confirmed by the SHG-weighted electron density²⁷ projected onto the constituted groups as displayed in Figure 4. In virtual electron

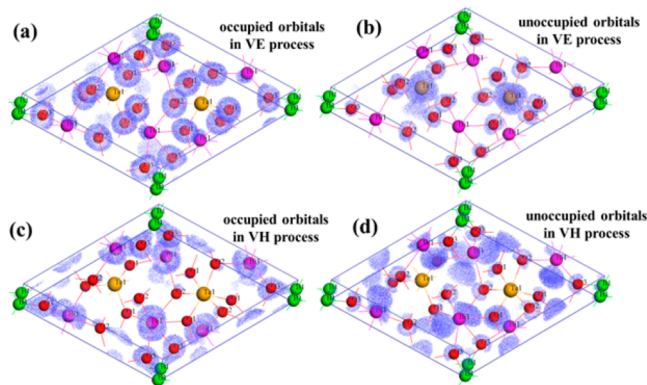


Figure 4. SHG-weighted electron densities of the (a) occupied and (b) unoccupied orbitals virtual electron process, (c) occupied and (d) unoccupied orbitals virtual hole process. The Bi, Te, B, and O atoms are represented by Indian red, yellow, green, and red balls, respectively.

(VE) process the majority of electron densities contributing to SHG effect are concentrated on the orbitals of TeO₆ octahedra (Figure 4a,b), despite a small amount on the lone pair electrons of bismuth in BiO₆ octahedra. In comparison, the SHG densities in virtual hole (VH) process mainly arises from the orbitals of BiO₆ and BO₃ groups, and the SHG densities on BiO₆ octahedra are much more than those on BO₃ triangles (Figure 4c,d). As the VE process has dominant contribution to the overall SHG effect,²⁷ TeO₆ octahedra may play a major role in the enhancement of the SHG response in BTBO.

Until now, the only other known NLO material that includes all the three types of NLO-active units is BiCd₄O(BO₃)₃.²⁸ This material contains the SOJT polyhedra CdO_n ($n = 6, 7$), SCALP BiO₆, and π -orbital planar BO₃ groups simultaneously, and also exhibits a very large SHG response (about 6 times that of KDP). Clearly, the magnitude of SHG effect in BTBO is much larger than that of BiCd₄O(BO₃)₃. It is well-known that the SHG response is dominantly determined by the ability to produce induced dipole moments when subjected to external optical electric field.²⁹ The “flexibility index” (F) has been defined to characterize quantitatively the ability to generate induced dipole moment of the concerning groups based on the bond-valence concept, according to which the SHG susceptibility is positively correlated to the F index of the group.³⁰ The F index of TeO₆ octahedron in BTBO is calculated to be 0.152, which is almost the same as the values in Pb₃MTe₃X₂O₁₄ ($M = \text{Zn, Mg; } X = \text{P, V}$), a series of recently discovered NLO materials with large SHG effect¹⁷ (Table S5). In comparison, the F indices of CdO_n ($n = 6, 7$) polyhedra in BiCd₄O(BO₃)₃ are less than 0.120. Thus, the TeO₆ units are easier to generate larger induced dipole moment and contribute more to macroscopic SHG response of crystal compared with the CdO_n ($n = 6, 7$) groups (also see Table S5 and Discussion S2). In addition, the number ratio of (BiO₆+TeO₆):BO₃ in BTBO is larger than that of (BiO₆+CdO_n):BO₃ in BiCd₄O(BO₃)₃. Therefore, the introduction of more “flexible” TeO₆ octahedra and the high number proportion of BiO₆ and TeO₆ groups

synergistically result in the much larger SHG effect of BTBO in comparison with BiCd₄O(BO₃)₃.

The UV–vis–NIR diffuse reflectance spectrum indicated that BTBO exhibits high transmittance in the range of 500–2500 nm with a UV absorption edge at 385 nm, manifesting that BTBO is a promising NLO crystal in the visible to near UV range (Figure S7). In addition, BTBO crystal possesses a high density (7.72 g/cm³), which is beneficial for a scintillating material. Compared to the commercial scintillators such as Bi₄Si₃O₁₂ (BSO) (6.7 g/cm³), Bi₄Ge₃O₁₂ (BGO) (7.13 g/cm³), and (Lu_{1-x}Y_x)₂SiO₅ (LYSO) (about 7.3 g/cm³), BTBO with higher density may also be used in the potential applications in high energy physics, medical imaging, and security check.

In summary, we have successfully designed a new polar crystal Bi₃TeBO₉ with three NLO-active units including SCALP cation BiO₆, distorted TeO₆ octahedron, and π -orbital planar BO₃ group in the structure. The title compound features an enhanced strong SHG response of 20 times that of KDP, showing the largest SHG effect among the ever-reported borate NLO crystals. First-principles analysis reveals that the large SHG response resulted from the synergistic effect of constituted NLO-active groups. We postulate that BTBO crystal may be employed as a promising NLO material for SHG application for its large NLO coefficients and high symmetry (for convenience), and that the “all-three-in-one” strategy adopted in the present work would have great implications on the search and design of new NLO materials with large SHG effects.

■ ASSOCIATED CONTENT

📄 Supporting Information

The Supporting Information is available free of charge on the ACS Publications website at DOI: 10.1021/jacs.6b08813.

Experimental and calculated methods, DSC curves, diffuse reflectance spectra, calculated electronic structures and relevant discussion, flexibility indices F for groups, and additional data (PDF)

Crystallographic data (CIF)

■ AUTHOR INFORMATION

✉ Corresponding Author

*zslin@mail.ipc.ac.cn rkli@mail.ipc.ac.cn

Notes

The authors declare no competing financial interest.

■ ACKNOWLEDGMENTS

This work was financially supported by the National Natural Science Foundation of China (Grant No. 51502307), National Instrumentation Program (No. 2012YQ120048), and China “863” project (No. 2015AA034203). We also thank Mr. Lei Xiao and Dr. Sangen Zhao for help with the powder SHG test and useful discussion.

■ REFERENCES

- (1) (a) Partanen, J. *Opt. Photonics News* **2002**, *13*, 44. (b) Norreys, P. A.; Zepf, M.; Moustazis, S.; Fews, A. P.; Zhang, J.; Lee, P.; Bakarezos, M.; Danson, C. N.; Dyson, A.; Gibbon, P.; Loukakos, P.; Neely, D.; Walsh, F. N.; Wark, J. S.; Dangor, A. E. *Phys. Rev. Lett.* **1996**, *76*, 1832.
- (2) (a) Baumgart, P.; Krajnovich, D. J.; Nguyen, T. A.; Tam, A. G. *IEEE Trans. Magn.* **1995**, *31*, 2946. (b) Gu, B.; Schramm, R.; Gillespie, J.; Mezack, G.; Cunningham, A. *IMAPS North America*, 2003.

- (3) (a) Munn, R. W.; Ironside, C. N. *Principles and Applications of Nonlinear Optical Materials*; CRV Press Inc.: Boca Raton, FL, 1993. (b) Nikogosyan, D. N. *Nonlinear Optical Crystals: A Complete Survey*; Springer Press Inc.: New York, 2005.
- (4) Boyd, G. D.; Kasper, H.; McFee, J. H. *IEEE J. Quantum Electron.* **1971**, *7*, 563.
- (5) Boyd, G. D.; Kasper, H. M.; McFee, J. H.; Storz, F. G. *IEEE J. Quantum Electron.* **1972**, *8*, 900.
- (6) Boyd, G. D.; Buehler, E.; Storz, F. G. *Appl. Phys. Lett.* **1971**, *18*, 301.
- (7) Haussühl, S. Z. *Kristallogr.* **1964**, *120*, 401.
- (8) (a) Jacco, J. C. *Proc. SPIE* **1988**, *968*, 93. (b) Bierlein, J. D. *Proc. SPIE* **1989**, *1104*, 2.
- (9) Chen, C. T.; Wu, B. C.; Jiang, A. D.; You, G. M. *Sci. Sin., Ser. B* **1985**, *28*, 235.
- (10) Chen, C. T.; Wu, Y. C.; Jiang, A. D.; Wu, B. C.; You, G. M.; Li, R. K.; Lin, S. J. *J. Opt. Soc. Am. B* **1989**, *6*, 616.
- (11) (a) Tu, J. M.; Keszler, D. A. *Mater. Res. Bull.* **1995**, *30*, 209. (b) Mori, Y.; Kuroda, I.; Nakajima, S.; Sasaki, T.; Nakai, S. *Appl. Phys. Lett.* **1995**, *67*, 1818.
- (12) Chen, C. T.; Wang, Y. B.; Xia, Y. N.; Wu, B. C.; Tang, D. Y.; Wu, K. C.; Wenrong, Z.; Yu, L. H.; Mei, L. F. *J. Appl. Phys.* **1995**, *77*, 2268–2272.
- (13) (a) Halasyamani, P. S.; Poeppelmeier, K. R. *Chem. Mater.* **1998**, *10*, 2753. (b) Halasyamani, P. S. *Chem. Mater.* **2004**, *16*, 3586. (c) Huang, Y. Z.; Wu, L. M.; Wu, X. T.; Li, L. H.; Chen, L.; Zhang, Y. F. *J. Am. Chem. Soc.* **2010**, *132*, 12788.
- (14) (a) Huang, H. W.; Yao, J. Y.; Lin, Z. S.; Wang, X. Y.; He, R.; Yao, W. J.; Zhai, N. X.; Chen, C. T. *Angew. Chem., Int. Ed.* **2011**, *50*, 9141. (b) Huang, H. W.; Liu, L. J.; Jin, S. F.; Yao, W. J.; Zhang, Y. H.; Chen, C. T. *J. Am. Chem. Soc.* **2013**, *135*, 18319. (c) Wu, H. P.; Yu, H. W.; Yang, Z. H.; Hou, X. L.; Su, X.; Pan, S. L.; Poeppelmeier, K. R.; Rondinelli, J. M. *J. Am. Chem. Soc.* **2013**, *135*, 4215. (d) Zhao, S. G.; Gong, P. F.; Bai, L.; Xu, X.; Zhang, S. Q.; Sun, Z. H.; Lin, Z. S.; Hong, M. C.; Chen, C. T.; Luo, J. H. *Nat. Commun.* **2014**, *5*, 4019.
- (15) (a) Dong, X. Y.; Jing, Q.; Shi, Y. J.; Yang, Z. H.; Pan, S. L.; Poeppelmeier, K. R.; Young, J.; Rondinelli, J. M. *J. Am. Chem. Soc.* **2015**, *137*, 9417. (b) Cao, X. L.; Hu, C. L.; Xu, X.; Kong, F.; Mao, J. G. *Chem. Commun.* **2013**, *49*, 9965.
- (16) (a) Baucher, A.; Gasperin, M. *Mater. Res. Bull.* **1975**, *10*, 469. (b) Nicholls, J. F. H.; Henderson, B.; Chai, B. H. T. *Opt. Mater.* **1997**, *8*, 215.
- (17) (a) Yu, H. W.; Zhang, W. G.; Young, J.; Rondinelli, J. M.; Halasyamani, P. S. *J. Am. Chem. Soc.* **2016**, *138*, 88. (b) Yu, H. W.; Young, L.; Wu, H. P.; Zhang, W. G.; Rondinelli, J. M.; Halasyamani, P. S. *J. Am. Chem. Soc.* **2016**, *138*, 4984.
- (18) (a) Ra, H. S.; Ok, K. M.; Halasyamani, P. S. *J. Am. Chem. Soc.* **2003**, *125*, 7764. (b) Zhang, J. J.; Zhang, Z. H.; Zhang, W. G.; Zheng, Q. X.; Sun, Y. X.; Zhang, C. Q.; Tao, X. T. *Chem. Mater.* **2011**, *23*, 3752. (c) Zhang, J. J.; Zhang, Z. H.; Sun, Y. X.; Zhang, C. Q.; Tao, X. T. *CrystEngComm* **2011**, *13*, 6985. (d) Zhang, W. G.; Tao, X. T.; Zhang, C. Q.; Gao, Z. L.; Zhang, Y. Z.; Yu, W. T.; Cheng, X. F.; Liu, X. S.; Jiang, M. H. *Cryst. Growth Des.* **2008**, *8*, 304. (e) Fuks-Janczarek, L.; Miedzinski, R.; Brik, M. G.; Majchrowski, A.; Jaroszewicz, L. R.; Kityk, I. V. *Solid State Sci.* **2014**, *27*, 30.
- (19) (a) Chang, H. Y.; Kim, S. H.; Halasyamani, P. S.; Ok, K. M. *J. Am. Chem. Soc.* **2009**, *131*, 2426. (b) Chang, H. Y.; Kim, S. H.; Ok, K. M.; Halasyamani, P. S. *J. Am. Chem. Soc.* **2009**, *131*, 6865.
- (20) Sun, C. F.; Hu, C. L.; Xu, X.; Ling, J. B.; Hu, T.; Kong, F.; Long, X. F.; Mao, J. G. *J. Am. Chem. Soc.* **2009**, *131*, 9486.
- (21) (a) Zou, G. H.; Huang, L.; Ye, N.; Lin, C. S.; Cheng, W. D.; Huang, H. J. *J. Am. Chem. Soc.* **2013**, *135*, 18560. (b) Tran, T. T.; Halasyamani, P. S.; Rondinelli, J. M. *Inorg. Chem.* **2014**, *53*, 6241.
- (22) Steele, W.; Decius, J. J. *Chem. Phys.* **1956**, *25*, 1184.
- (23) Kurtz, S. K.; Perry, T. T. *J. Appl. Phys.* **1968**, *39*, 3798.
- (24) (a) Kohn, W.; Sham, L. J. *Phys. Rev.* **1965**, *140*, A1133. (b) Payne, M. C.; Teter, M. P.; Allan, D. C.; Arias, T. A.; Joannopoulos, J. D. *Rev. Mod. Phys.* **1992**, *64*, 1045.
- (25) Palik, E. D. *Handbook of Optical Constants of Solids*; Academic Press: New York, 1985.
- (26) (a) Lin, J.; Lee, M. H.; Liu, Z. P.; Chen, C. T.; Pickard, C. J. *Phys. Rev. B: Condens. Matter Mater. Phys.* **1999**, *60*, 13380. (b) Lin, Z. S.; Lin, J.; Wang, Z. Z.; Lee, M. H.; Chen, C. T. *Phys. Rev. B: Condens. Matter Mater. Phys.* **2000**, *62*, 1757.
- (27) (a) Lee, M. H.; Yang, C. H.; Jan, J. H. *Phys. Rev. B: Condens. Matter Mater. Phys.* **2004**, *70*, 235110. (b) He, R.; Lin, Z. S.; Lee, M. H.; Chen, C. T. *J. Appl. Phys.* **2011**, *109*, 103510.
- (28) Zhang, W. L.; Cheng, W. D.; Zhang, H.; Geng, L.; Lin, C. S.; He, Z. Z. *J. Am. Chem. Soc.* **2010**, *132*, 1508.
- (29) Butcher, P. N.; Cotter, D. *The Elements of Nonlinear Optics*; Cambridge University Press: Cambridge, 1990.
- (30) Jiang, X. X.; Zhao, S. G.; Lin, Z. S.; Luo, J. H.; Bristowe, P. D.; Guan, X. G.; Chen, C. T. *J. Mater. Chem. C* **2014**, *2*, 530.